

THz Emission Characteristics of Photoconductive Antennas with Different Gap Size Fabricated on Arsenic-Ion-Implanted GaAs

Tze-An Liu^a, Masahiko Tani^b, Gong-Ru Lin^c and Ci-Ling Pan^a

^aInstitute of Electro-Optic Engineering, National Chiao Tung University 1001 Ta-Hsueh Rd., Hsinchu, Taiwan 300, R.O.C.

^bKansai Advanced Research Center, Communications Research Laboratory, Ministry of Posts and Telecommunications, 588-2 Iwaoka, Nishi-ku, Kobe, Hyogo 651-2401, Japan.

^cInstitute of Electro-Optic Engineering, Tatung University, 40 Chung Shan N Rd, Sect 3, Taipei 10451, Taiwan.

ABSTRACT

Significant difference in temporal and spectral characteristics of THz radiation emitted by large- (1mm) and small- (5 μ m) aperture dipole antennas fabricated on arsenic-ion-implanted GaAs and undoped semi-insulating GaAs is reported and attributed to the geometry of the antenna.

Keywords: THz radiation, Arsenic-ion-implanted GaAs, Large-aperture photoconductive antenna, dipole antenna.

1. INTRODUCTION

Optically-excited THz radiation from semiconductors has been extensively studied in the past decade¹⁻². For example, large aperture photoconductive³ or small gap dipole antennas⁴ fabricated on semi-insulated GaAs (S.I. GaAs) and low-temperature MBE-grown GaAs (LT-GaAs) had been investigated as THz emitters. LT-GaAs has been the premiere photoconductor for ultrafast optoelectronic applications. Recently an alternative arsenic-rich-material, arsenic-ion-implanted GaAs, or GaAs:As⁺, has emerged as a potential candidate for ultrafast optoelectronic applications.⁵ After annealing, the high break down voltage and good mobility makes it a candidate for generating higher THz radiation power by applying larger electric field. The amplitude of THz radiation is related with carrier mobility, bias field, pumping power and gap size. THz spectrum is mainly related from rise time (which is dominated by laser pulse width) and recovery time (which is from carrier scattering, carrier trapping time carrier recombination and transient time). Material searching for the high mobility, high resistance for high break down voltage, low dark current and short carrier response time is very important. In this paper, we report for the first time emission characteristics of variant gap size photoconductive antennas fabricated on Arsenic-ion-implanted GaAs (GaAs:As⁺). Their performances are compared to

those of similar devices made of S. I. GaAs.

2. EXPERIMENTAL

In a first series of experiments, we study the characteristics of large-aperture photoconductive antennas (LAPA) of gap sizes of 0.7mm and 0.8mm fabricated on GaAs:As⁺. The devices studied include single-energy (200 KeV) implanted GaAs:As⁺ at dosages of 10¹⁶ and 10¹⁵ ions/cm² and furnace annealed at 600°C with 30min processing. These were operated at bias voltages of 200V and 310V, respectively. LAPA's were also fabricated on multiple-energy-implanted (50, 100, 200keV) GaAs:As⁺ at a dosage of 10¹⁵ ions/cm², (also with furnace annealed at 600°C with 30min processing) a gap size of 0.7mm and operated at a bias voltage of 310V. S.I.-GaAs-based LAPA with 0.5mm gap and biased at 75V was used for comparison. The antenna consists two coplanar strip lines with Au metallic coating layers of 300nm. For the break down voltage measurement with fabricated to the CPW structure with gap size of 20um, although the dark current of GaAs:As⁺ is comparable with S.I. GaAs of about sub nA in low bias voltage, the break down voltage of 240V is higher than the S.I. GaAs of 60V with about 4 times larger. Figure 1 shows the transient reflectance changes ($\Delta R/R$) for the samples. It was performed by a pump-probe system using wavelength of 840nm and pulse width of 150fs laser pulses produced from a mode-locked Ti:sapphire laser. From the carrier lifetime measurement, the comparison with S.I. GaAs is shown in fig.1. By fitting multiple exponentials to the photorefectance decay curves, the carrier lifetime of multi-GaAs:As⁺ and S.I. GaAs is estimated to around 1ps and 150ps.

Optically-excited THz signals were collimated and focused onto the EO sensor of ZnTe with thickness of 1.5mm by a pair of paraboloidal mirrors. Since the THz radiation was collected by parabolic mirrors in this experiment, the temporal resolution would be limited by group velocity mismatch between the optical probe beam and THz radiation⁶. The LAPAs were excited by average power of 300 mW and pulse width of 130fs Ti : sapphire laser. The wavelength and repetition rate are respectively 785nm and 87MHz. The ZnTe crystal for EO detection is 1.5mm in thickness.

In a second series of experiments, the gap size of small gap dipole antennas (SGDA) is about 5 μ m. The samples are fabricated on S.I.-GaAs or multiple-energy-implanted (50, 100, 200keV) GaAs:As⁺ at a dosage of 10¹⁵ ions/cm² with furnace annealed at 600°C with 30min processing. The devices are operated at a bias voltage of 10V. The pumping source is a commercial Ti:sapphire oscillator with average power of 5mW at repetition rate of 82MHz with pulse width of 80fs and wavelength of 780nm. Photoconductive detection with dipole antenna fabricated in annealed LT-GaAs with gap size of 5 μ m was used in this series of experiments.

3. RESULTS AND DISCUSSIONS

Comparison of THz radiation waveform and spectrum between S.I. GaAs and single or multi energy implanted GaAs:As⁺ fabricated antennas with gap size of around 0.8mm are shown in Figure 2. The center frequencies of the THz radiation

from the LAPA's are all around 0.4 THz and the spectral widths are about 0.8 THz. The temporal waveforms are all symmetric bipolar. The emission characteristics of LAPA's fabricated on S. I. GaAs and GaAs:As⁺ are quite similar. The THz radiation waveform by LAPA with different gap spacing had been previously studied by G. Rodriguez et al⁷. Bipolar waveform can be explained from space charge screening of the bias field, but the larger gap spacing (larger than 5mm) will diminishes the effect. Although waveforms are all symmetric bipolar, there are still not so obviously different between these two kind of materials even with the variant Arsenic ion implantation situation. The probably reason is that: the skin depth of pumping laser is about 800nm, which is larger than the depth of As ion implantation region(~100nm). Besides that, the bias field maybe has a large part of electric field penetrate into the perpendicular direction than the transverse one in the large aperture photoconductive antenna.

The THz waveform and the corresponding spectrum emitted by the dipole antenna fabricated on multi-energy implanted GaAs:As⁺, biased at 10V and an optical excitation power of 5 mW are shown in Fig. 3. Asymmetric unipolar waveform is shown in S.I. GaAs. However, it changed to the bipolar in our GaAs:As⁺ material and reminiscent of that devices made on LT GaAs.⁴ The pronounced negative peak is attributed to the fast carrier trap time of GaAs:As⁺. In Fig. 3(b), we note that the center frequency in GaAs:As⁺ fabricated antenna has shifted from 0.7 THz to 0.9 THz compared to S.I. GaAs one while the band width is around 1.2 THz. As in the small gap situation, the electric field will have larger component in the transverse direction which will mostly effect the As ion implanted region. The obviously difference between large gap and small gap antenna can be explained by this reason.

Fig. 4 shows the THz radiation waveform with different gap size photoconductive antennas fabricated in (a) S.I. GaAs and (b) GaAs: As⁺. Although the detection scheme is different, the waveform in S.I. GaAs is significantly different between these two devices.

4. CONCLUSION

In summary, we have compared the THz emission characteristics of large-aperture photoconductive antennas and small-gap dipole antennas fabricated on multi-energy implanted GaAs:As⁺ and S. I. GaAs, for the first time to our knowledge. For the small-gap antenna, the distinction is apparent. This is, however, not the case for large-aperture photoconductive antennas, of which the performance is dominated mostly by the characteristics of the bulk S.I. GaAs substrate. Further improvement with blocking layer of electric field between bulk GaAs and implanted region in LAPA should increase the effect of generating THz radation from GaAs:As⁺.

REFERENCES

1. X. -C. Zhang and D. H. Auston, "Optoelectronic measurement of semiconductor surfaces and interfaces with femtosecond optics," *J. Appl. Phys.*, vol. 71, pp. 326-338, 1992.
2. P. C. M. Planken, M. C. Nuss, W. H. Knox, D. A. B. Miller and K. W. Goossen, "THz pulses from the creation of polarized electron-hole pairs in biased quantum wells," *Appl. Phys. Lett.*, vol. 61, pp 2009-2011, 1992.
3. S. G. Park, A. M. Weiner, M. R. Melloch, C. W. Siders, J. L. W. Siders and A. J. Taylor, "High-power narrow-band terahertz generation using large-aperture photoconductors," *IEEE J. Quantum. Electron.*, vol. 35, pp. 1257-1268, 1999.
4. M. Tani, S. Matsuura, K. Sakai, and S. Nakashima, "Emission characteristics of photoconductive antennas based on low-temperature-grown GaAs and semi-insulating GaAs," *Appl. Opt.*, vol. 36, pp. 7853-7859, 1997.
5. F. Ganikhanov, G. -R. Lin, W. C. Chen, C. S. Chang and C. -L. Pan, "Subpicosecond carrier lifetimes in arsenic-ion-implanted GaAs," *Appl. Phys. Lett.*, vol. 67, pp. 3465-3467, 1995.
6. Y. Cai, I. Brener, J. Lopata, J. Wynn, L. Pfeiffer, J. B. Stark, Q. Wu, X. C. Zhang and J. F. Federici, "Coherent terahertz radiation detection: Direct comparison between free-space electro-optic sampling and antenna detection," *J. Appl. Phys.*, vol. 73, pp. 444-446, 1998.
7. G. Rodriguez and A.J. Taylor, "Screening of the bias field in terahertz generation from photoconductors," *Opt. Lett.*, vol. 21, pp. 1046-1048, 1996.

FIGURE CAPTIONS

Fig.1 Transient photoreflectance changes for S.I. GaAs(solid circle) and multi-GaAs:As⁺(open circle).

Fig.2 (a) THz radiation pulses from large aperture (~mm order) photoconductive antenna fabricated on multi-implant GaAs:As⁺ (solid curve) with variant implant energy and S.I.GaAs (dashed curve).(b) Fourier-transformed amplitude spectrum of (a)

Fig.3 (a) THz radiation pulses from small gap (~μm order) photoconductive antenna fabricated on multi-implant GaAs:As⁺ (solid curve) and S.I.GaAs (dashed curve).(b) Fourier-transformed amplitude spectrum of (a)

Fig.4 THz radiation waveform with different gap size photoconductive antennas fabricated in (a) S.I. GaAs and (b) GaAs: As⁺

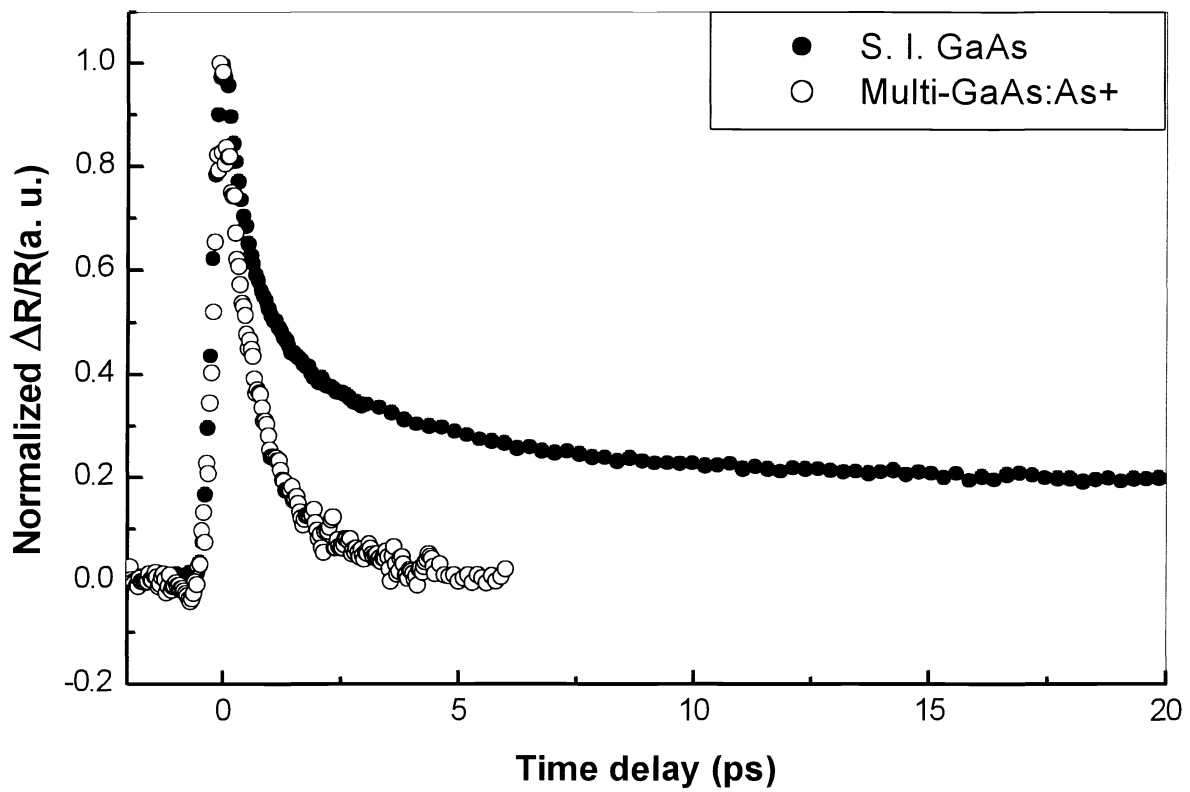


Fig.1 Transient photoreflectance changes for S.I. GaAs(solid circle) and multi-GaAs:As⁺(open circle).

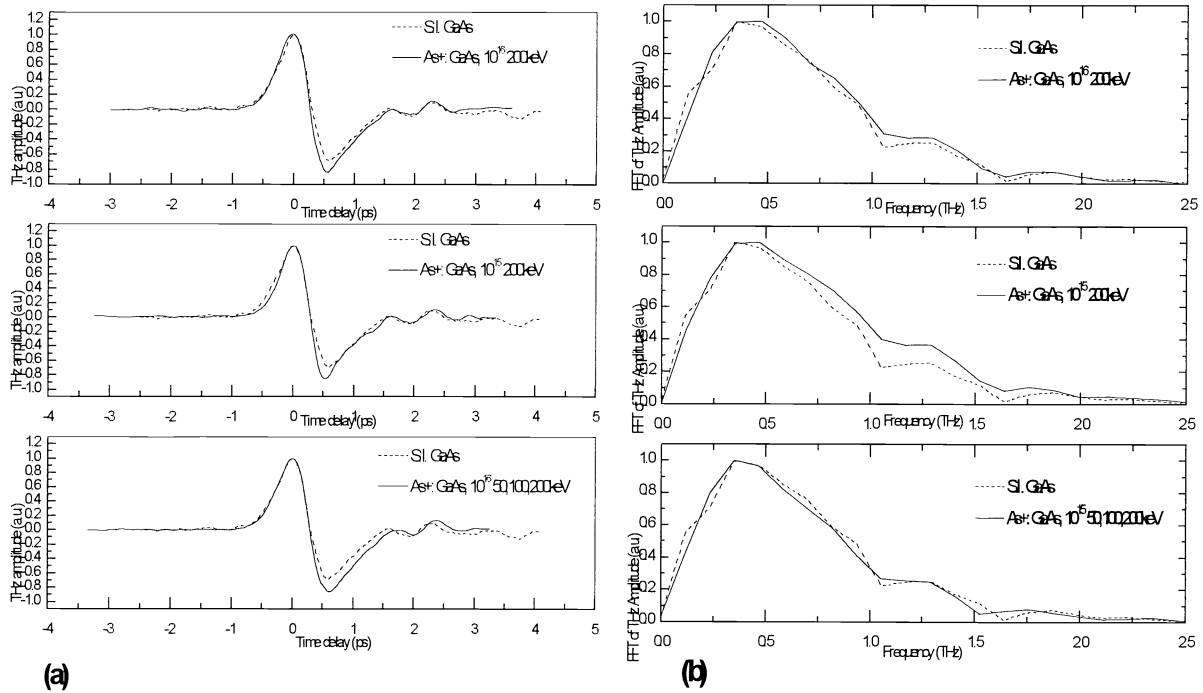


Fig.2 (a) THz radiation pulses from large aperture (\sim mm order) photconductive antenna fabricated on multi-implant GaAs:As+ (solid curve) with variant implant energy and S.I.GaAs (dashed curve).(b) Fourier-transformed amplitude spectrum of (a)

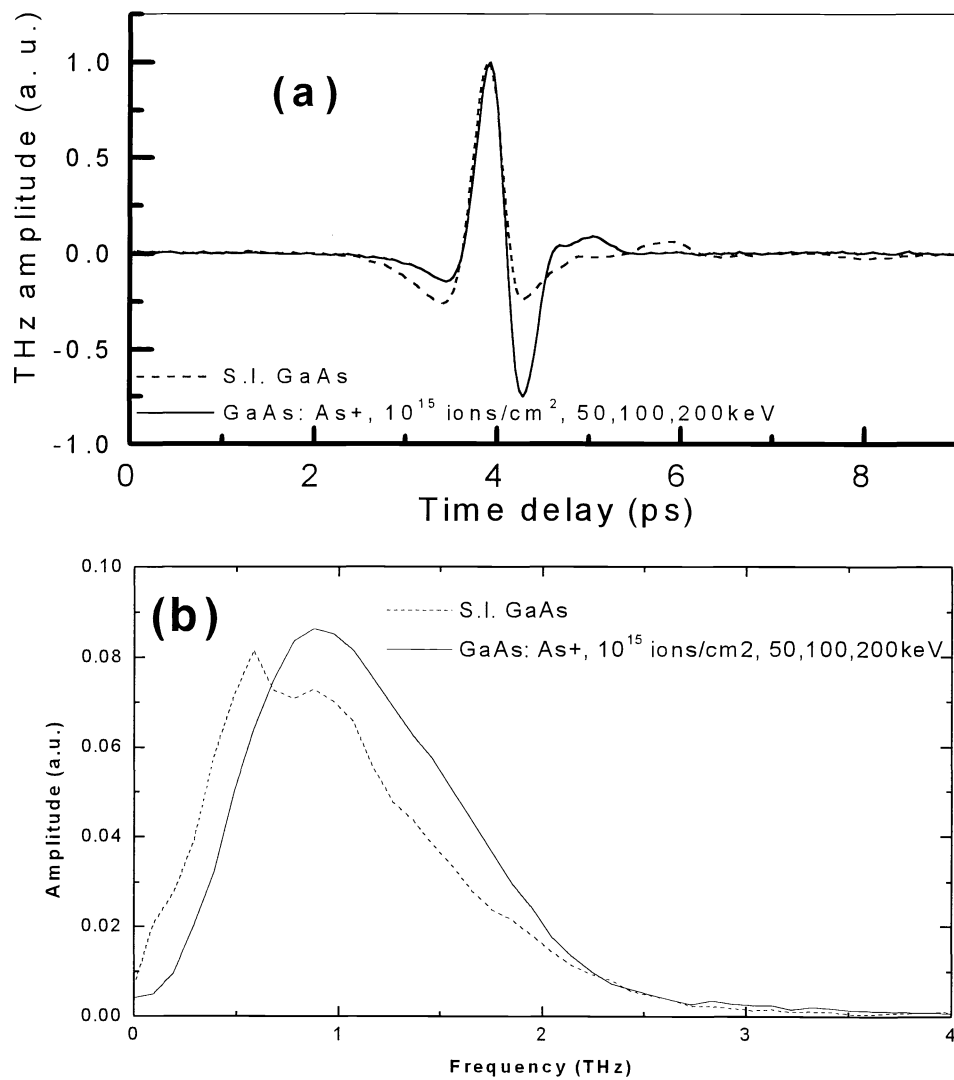


Fig.3 (a) THz radiation pulses from small gap ($\sim\mu\text{m}$ order) photconductive antenna fabricated on multi-implant GaAs:As+ (solid curve) and S.I.GaAs (dashed curve).(b) Fourier-transformed amplitude spectrum of (a)

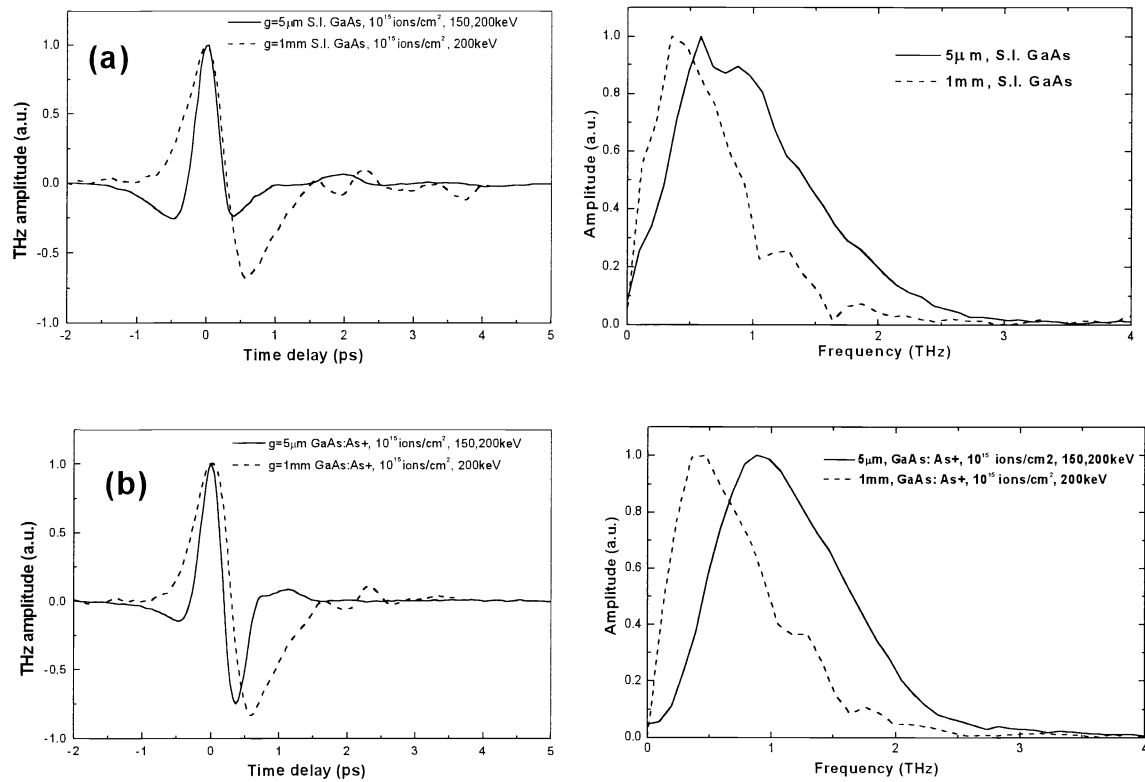


Fig.4 THz radiation waveform with different gap size photoconductive antennas fabricated in (a) S.I. GaAs and (b) GaAs: As+